

Gel-Combustion Synthesized Vanadium pentoxide Nanowire Clusters as Cathode Material for Rechargeable Lithium-Ion Batteries

Alamelu.K. Ramasami^{a,b}, M. V. Reddy^{b,c}, P. Nithyadharseni^{b,d}, B. V. R. Chowdari^b, Geetha. R. Balakrishna^{a,*}

^a Centre for Nano and Material Sciences, Jain University, Bangalore -562117, India.

^b Advanced Batteries Lab, National University of Singapore- 117546, Singapore.

^cDepartment of Materials Science and Engineering, National University of Singapore, Singapore 117576, Singapore

^dEnergy Materials, Materials Science and Manufacturing, Council for Scientific and Industrial Research (CSIR), Pretoria 0001, South Africa

Abstract

Gel-combustion by a bio-fuel, processed starch of the root tuber of cassava (*Manihot esculenta*), was used to prepare vanadium pentoxide nanowire clusters (V_2O_5 NWC). The as-synthesized product was characterized by X-ray diffraction (XRD), Scanning electron microscopy (SEM), Transmission electron microscopy (TEM), Fourier transform infrared spectroscopy (FTIR) UV-Visible spectroscopy and Photoluminescence (PL) spectroscopy. The electrochemical performance of V_2O_5 NWC has been evaluated by cyclic voltammetry (CV), galvanostatic cycling (GC) and electrochemical impedance spectroscopy (EIS). The V_2O_5 NWC had a discharge capacity of 188 mAhg^{-1} with better capacity retention of 90% at the end of the 50th cycle, which corresponds to a coulombic efficiency of around 99%. The rate performance of the compound is also carried out and it has shown excellent performance. EIS was used to study the kinetic properties of Li^+ ions for V_2O_5 NWC and the fitted resistance and capacitance values are discussed in detail.

Keywords: Vanadium pentoxide, nanowire clusters, gel-combustion, cassava starch, lithium-ion batteries

* Corresponding Author: E-mail address: br.geetha@jainuniversity.ac.in

1. Introduction

Nanocrystalline transition metal oxides (TMOs) have been the topic of research for decades due to their technological applications like lithium-ion batteries, photocatalytic degradation, etc. and fundamental aspects like surface-to-volume ratio, increased chemical reactivity, special optical properties and exceptional electronic properties [1]. TMOs find application in various fields like catalysis [2], electrochromism [3], energetics [4] and energy storage [5]. To mitigate the energy crisis, various advanced techniques like photovoltaic cells, energy from nuclear reactors and wind have been identified as alternate power sources. For storage of the energy thus generated, lithium ion batteries are, indeed, becoming attractive, especially, for electric vehicles/hybrid vehicles and power grid due to their remarkable energy and power density [6]. Since 1991, these lithium ion batteries have come a long way and have become an important energy storage technique. Oxides of Ni, Fe, Co, Ti, Mn, Cu, Cr, [7], Mo [8] and V [9] have been used as electrode materials for lithium ion batteries so far. Amongst these oxides of vanadium [10-12], especially V_2O_5 , has been used as cathode material in secondary batteries because of its high theoretical capacity (440 mAhg^{-1}), easy synthesis and low cost [13]. However, poor electronic conductivity and low diffusion coefficient of this material pose difficulties in their practical application. Nevertheless, these issues can be redressed by using nanostructured vanadia to reduce the diffusion distance and composites of the metal oxide with conductive materials for better electron conductivity [14]. Moreover, V_2O_5 has a typical layered structure and crystalline lattice allowing reversible

intercalation of mobile guest species (3 Li^+) into its appropriately- sized empty sites and thereby, conserving the structural integrity [15, 16].

In literature, various efforts on improvement in the morphology of vanadium pentoxide, that determine the efficiency of the cathode material, have been recorded [17-19]. Ng et al. [18] had used 1-D V_2O_5 with improved crystalline structures by varying the annealing temperature where the voltage range was 1.5-4V with a current density of 50 mA g^{-1} for better battery performance (200 mA h g^{-1} after 20 cycles; initial discharge capacity $>300 \text{ mA h g}^{-1}$). Zhu et al. had synthesized hollow microspheres of V_2O_5 by self-assembly method which had an initial capacity of 319 mA h g^{-1} and 160 mA h g^{-1} after 45 cycles. [19]. Though many techniques like hydrothermal [20], solvo-thermal [21], precipitation [22], sol-gel [23] polymer precursor method [24], chemical vapour deposition [25], Rf-Magnetron sputtering [26] and anodisation in commercial fish-water electrolyte [27] are used for the synthesis of vanadium pentoxide nanostructures, combustion method has been adopted in this present work to synthesise vanadium pentoxide nanowire clusters ($\text{V}_2\text{O}_5\text{NWC}$) due the advantages of the method: simple, cost-effective equipments and raw materials, homogeneous and crystalline product in few minutes [28]. Combustion synthesis involves evaporation of the metal salt solution (precursor) and an organic complexing agent, called fuel or oxidizer (cassava starch, in the present work) which forms an oxidizer-precursor gel. The gel on ignition gives the product with the removal of organic matter [29]. Combustion synthesis has been employed for the synthesis of SnO_2 nanowires [30], SiC nanowires [31], NiO nanoparticles [32], ZnCo_2O_4 [33] and InVO_4 [34]. Bio-fuels like commercial starch [35], corn starch [36], a combination of triethanolamine and starch [37] have been used to synthesise various nanoparticulates. The use of different types of fuels like urea [38], ethyl nitrate, ammonium nitrate and citric acid [39] have been recorded by different research groups for the synthesis of V_2O_5 nanoparticles by combustion method. Inspired by these

reports [38, 39], cassava starch derived from tapioca pearls (*Manihot esculenta*) has been used as a fuel in this work. Any fuel, that is efficient, should be rich in carbohydrates to support combustion. Cassava was chosen over the other starchy materials like potato and corn due to its higher starch content [40]. Furthermore, cassava pearls are natural, cheap, readily available in the market and abundant. Gel/solution combustion syntheses usually yield nanopowders or particulates [A. Jagadeesh, T.M. Rattan, M. Muralikrishna, K. Venkataramaniah, 'Instant one step synthesis of crystalline nanoV₂O₅ by solution combustion method showing enhanced negative temperature coefficient of resistance', Materials Letters 121, 2014, 133–136.

Z.Cao, M. Qin, B. Jia, Y. Gu, P. Chen, A. A. Volinsky, X. Qu, 'One Pot Solution Combustion Synthesis of Highly Mesoporous Hematite for Photocatalysis', Ceramics International 41, 2015, 2806-2812.]

and this is the first time a different morphology, nanowire clusters have been reported and to the best of our knowledge, it also the first one to report the synthesis of V₂O₅NWC by combustion method using cassava starch. The other noteworthy features of the method of synthesis are the simple and time-saving process, higher yield, use of naturally occurring fuel which doubles up as a template for the growth of nanowires.

2. Experimental Procedure

2.1. Preparation of V₂O₅NWC

The cassava starch has been prepared as described in our previous work [43]. Ammonium metavanadate (NH₄VO₃) (Merck) and cassava starch in the weight ratio of 1:0.5 (Also prepared 1:1 and 1:0.25 weight ratio of precursor to fuel, which resulted in a poor yield (blackish-grey) and was, hence, not studied further) were mixed well with 30 mL distilled water and heated on a hot plate at 200 °C till the mixture formed a semi-solid gel. This gel was introduced into a pre-heated muffle furnace at around 475 °C when smouldering type of

reaction occurred within 5 min along with the evolution of gases like water vapour, nitrogen and carbon dioxide, etc. A yellow V_2O_5 was formed which was further calcined at 500°C for 5 hours to remove the impurities that could have remained un-burnt.

2.2. Characterization

The structure of the synthesized V_2O_5 NWC was determined using Philips X'pert PRO X-ray diffractometer with graphite monochromatized $\text{Cu-K}\alpha$ (1541 \AA) radiation. Scanning electron microscope (SEM) (JEOL-JSM-6490 LV)(carried out by coating a thin layer of gold to avoid charging of the samples) and Transmission electron microscope (JEOL TEM 1200) operating at 120kV (samples were dispersed in alcohol, a drop of the sample was coated on carbon coated Cu grid) were used to study the morphology of the compound. FTIR spectrum was recorded by PerkinElmer FRONTIER FTIR spectrometer. The UV- Visible spectra were recorded by PerkinElmer lambda 750 spectrometer. Photoluminescence (PL) measurement was done using Shimadzu spectrofluorimeter (model RF 5301 PC) at 500 nm excitation.

2.3. Fabrication of batteries and coin cells for Lithium battery studies

The electrodes fabrication was carried out by mixing V_2O_5 NWC, polyvinylidene fluoride (PVDF), binder (Kynar 2801) and carbon black (NSACO, MMM Super P) a commercially available conductive carbon in 70:15:15 wt.%, respectively in N-methylpyrrolidinone (NMP) (Aldrich, 99% pure) solvent and stirred overnight. This electrode slurry was coated on Al foil by Doctor Blade technique and dried in a vacuum oven at 80°C , overnight. Then foil was cut into circular shape of 16 mm in diameter. The geometrical electrode area was around 2 cm^2 and mass of active material was 2–4 mg. The coin cells (CR2016) were assembled in Argon filled glove box (MBraun, Germany) using the

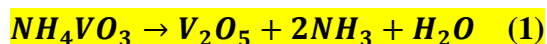
fabricated electrode as cathode, Li metal (Hohsen Corp., Japan, 99% pure) as counter/reference electrode and 1M LiPF₆ (lithium hexafluorophosphate) in ethylene carbonate (EC) and dimethyl carbonate (DMC) (1:1 by volume, Merck, Selectipur LP40) as electrolyte. Galvanostatic cycling (GC) and cyclic voltammetry (CV) were performed on the fabricated batteries by using Bitrode battery tester (model SCN, Bitrode, USA) and MacPile II (Biologic, France), respectively. The cycling test were carried out in the voltage range of 2.0-4.0 V vs. Li, at the current density of 60 mA g⁻¹ and CV was carried at the potential window of 2.0-4.0 V at a scan rate of 58 μV s⁻¹. Electrochemical Impedance Spectroscopic (EIS) measurement of the coin cell was done with a Solartron impedance/gain-phase analyser (model SI 1255) coupled with a potentiostat (SI 1268) at room temperature in the frequency range, 180000 - 0.003 Hz with an AC signal amplitude of 10 mV. The impedance data were analysed using Z-view software (version 2.2, Scribner Assoc., Inc. U.S.A.).

3. Results and discussion

3.1 Effect of Fuel and Mechanism of Nanowire clusters formation

Cassava starch plays three roles in the synthesis; 1) fuel, 2) seeding nuclei and 3) bio-temple. When cassava starch is heated above its gelatinization temperature (65 °C) [41], the hydrogen bonds present in the carbohydrates break and the liberated hydroxyl groups are attached to water molecules resulting in the swelling of the granules and these starch granules act as nuclei for the growth of nanoparticles. Once the nanoparticles attain certain size the starch strands act as template for the growth of V₂O₅ nanowire clusters [42] and on further heating acts as a fuel supporting combustion at higher temperatures.

Ammonium metavanadate on heating gives V₂O₅ according to the equation (1)[M. Taniguchi, T. R. Ingraham, Canadian Journal of Chemistry 42, 1964, 2467-2473.]



V_2O_5 nanoparticles formed are well dispersed in cassava starch gel. When this is further heated small nanoparticles disappear to give rise to larger ones by Oswald ripening process. With increase in temperature the larger nanoparticles grow on the starch template into wire like structures. This growth continues till all the nanoparticles are consumed and only nanowires are left. [M.R. Johan, N. A. K. Aznan, S. T. Yee, I. H. Ho, S. W. Ooi, N. D. Singho, F. Aplop, 'Synthesis and Growth Mechanism of Silver Nanowires through Different Mediated Agents ($CuCl_2$ and $NaCl$) Polyol Process', Journal of NanoMaterials 2014, DOI 10.1155/2014/105454.] The formation and growth of nanowires can be attributed to surface energy driven recrystallization process and surface migration (diffusion) of nanoparticles. These are the common phenomena that occur during growth of elongated nanomaterials from powders. The transformation of nanowires to nanowire clusters might have occurred during the calcination process. The merging of nanowires involves active surface migration and subsequent annihilation of grain boundaries and coalescence behaviour between the crystals of adjacent nanowires. [A. M. Glushenkov, V. I. Stukachev, M. F. Hassan, G. G. Kuvshinov, H. K. Liu, Y. Chen, 'A Novel Approach for Real Mass Transformation from V_2O_5 Particles to Nanorods', Crystal Growth and Design 8, 2008, 3661-3665.] Q. Song, H. Pang, W. Gong, G. Ning, S. Gao, X. Dong, C. Liu, J. Tian, Y. Lin, 'Fabrication of Nanostructured V_2O_5 via Urea Combustion for High Performance Li-ion Battery Cathode', RSC Adv. 5, 2015, 4256-4260.] The Schematic representation of the nanowire cluster formation is given in Fig.1

3.1. Structure and Morphology

Fig.2 shows the X-ray diffraction pattern of V_2O_5 NWC, which can be indexed to pure phase of orthorhombic V_2O_5 (Shcherbinaite), and the results are confirmed by JCPDS pattern (JCPDS No. 41-1426, with lattice parameters $a= 11.516$, $b= 3.565$, $c = 4.372$ Å with the space group $-pmmn$ 59) as well as the reported literature [44, 45]. The pattern also reveals the

absence of other impurities of V_xO_y phases or initial carbon residue and high purity of the sample.

The morphology of the V_2O_5 NWC prepared by gel-combustion method using cassava starch, as a fuel, has been evaluated by scanning electron microscope and transmission electron microscope, shown in Fig. 3 (a, b). The SEM image of V_2O_5 compound exhibits nanowire- clusters which are closely arranged. This preparation method resulted in different morphology of the material than those prepared by various other methods such as thermal decomposition [14], polymer precursor [24] and hydrothermal [46]. Thus may be attributed to the influence of cassava starch and the effect of preparation method. For better understanding of the morphology, TEM analysis has been done, which is shown in Fig. 3(b). The nanowires are in the range of 40-60 nm in diameter and found to occur as clusters.

The FT-IR spectrum of V_2O_5 NWC is given in Fig. 4. The vibrations between 500 to 1050 cm^{-1} can be attributed to V-O group. The band at 1007 cm^{-1} correspond to stretching vibrations of terminal oxygen bonds (V=O) [16] and 807 and 576 cm^{-1} bands ascribed to asymmetric and symmetric stretching vibrations of triply coordinated oxygen bonds in vanadia, respectively [47].

The UV- Visible reflectance spectrum of V_2O_5 NWC is presented in Fig. 5 (a). Presence of a broad peak at 410- 460 nm is due to the charge transfer transitions of V^{5+} species (V=O) [48]

Tauc's plot of V_2O_5 NWC is depicted in Fig. 5 (b) - (e). The optical absorption edge is determined by Tauc's equation [49],

$$\alpha h\nu = A(h\nu - E_g)^n \quad (1)$$

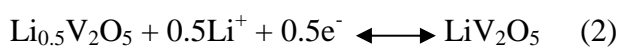
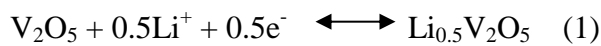
Where, A is a constant, $h\nu$ is photon energy, E_g is the energy gap, $n = 1/2$ for allowed direct transition, $n = 2$ for allowed indirect transition, $n = 2/3$ for forbidden direct transition and $n = 1/3$ for forbidden indirect transition [50]. The fundamental optical absorption edge in

vanadium pentoxide is quite complicated. V₂O₅ NWC exhibits all four probable transitions, namely, direct allowed with a band gap, 2.15 eV, indirect allowed transition with a band gap, 2.34 eV, direct forbidden transition with a band gap, 2.30 eV and indirect forbidden transition with a band gap, 2.38 eV. Though researchers have reported direct allowed transition with a band gap 2.2 eV [51], indirect forbidden transition with a band gap 2.32 [50], which lie close to the values reported in this article, the indirect band gap values deviate from them [52]. The reason for this anomalous behaviour, to the best of the literature review done, is still ambiguous.

The photoluminescence (PL) spectrum of V₂O₅ NWC is shown in Fig. 6. The PL spectrum displayed a broad emission spectrum in the visible region centred at 590 nm depicting oxygen defects [53] and this could be attributes to the V=O double bonds.

3.2 Electrochemical studies

Fig. 7 illustrates the cyclic voltammogram of V₂O₅NWC cycled in the voltage range of 2.0-4.0V vs. Li/Li⁺ at a scan rate of 58 μVs⁻¹. The cathodic and anodic peaks correspond to lithium-ion insertion and extraction process, respectively. There are three pairs of cathodic/anodic peaks in the range of 3.0-4.0 V and a pair of cathodic/anodic peak in the range 2.0-3.0 V. Apart from that few minor peaks were observed for V₂O₅NWC [24, 46]. The cathodic peaks in the 3.0-4.0V region indicate multi-step lithium ion insertion processes of the active material corresponding to phase changes from α-V₂O₅ to ε-Li_{0.5}V₂O₅(~ 3.3 V) to δ-LiV₂O₅(~ 3.2 V) as given in the equation 1 and 2.



The cathodic peak in the 2.0-3.0 V region is attributed to the intercalation of the second lithium ion, which corresponds to the phase transformation to γ-Li₂V₂O₅ (~ 2.2 V) from δ-LiV₂O₅ as represented in equation 3 [24].



During the anodic scan the reverse reactions take place along with the phase reversions. From the second to the sixth scan, the peak area and the intensity of the peaks are reduced which is due to minor fading of the compound.

The charge-discharge vs. voltage profile of V_2O_5 NWC is shown in Fig. 8 with a few selected cycles of 1, 5, 10, 20 and 30, cycled in the range of 2.0-4.0 V, at the current density of 60 mA g^{-1} . The plateau around at 3.5, 3.4, 3.1 and 2.4 V in the discharge curve correspond to lithium ion intercalation i.e., the phase transition from $\alpha\text{-V}_2\text{O}_5$ to $\epsilon\text{-Li}_{0.5}\text{V}_2\text{O}_5$, $\delta\text{-LiV}_2\text{O}_5$ and $\gamma\text{-Li}_2\text{V}_2\text{O}_5$, while the plateau in the charge curve correspond to de-intercalation of lithium ion and a reverse phase transition from $\gamma\text{-Li}_2\text{V}_2\text{O}_5$, $\delta\text{-LiV}_2\text{O}_5$, $\epsilon\text{-Li}_{0.5}\text{V}_2\text{O}_5$ and $\alpha\text{-V}_2\text{O}_5$ [14, 53]. These results are in good agreement with the CV scan. Moreover, these phase transitions are reversible even in subsequent cycles indicating the good reversibility of the compound, without the formation of rock-salt phase of $\omega\text{-Li}_3\text{V}_2\text{O}_5$ [14, 54]. The V_2O_5 NWC exhibited an initial discharge and charge capacity of 209 and 206 mAhg^{-1} with the corresponding coulombic efficiency of 96 % and the obtained discharge capacity at 30th cycle is 198 mAhg^{-1} . The discharge capacity fading was found be negligible (with less fading rate 0.1 % of per cycle) from the beginning to 50th cycle. The capacity retention at 30th cycle is 95 % with respect to the first cycle capacity. V_2O_5 NWC, synthesized by gel-combustion using cassava starch, is found to have high capacity with negligible capacity fading compared to other reports [44, 46, 47].

Cycle number vs. specific capacity and the corresponding coulombic efficiency of the V_2O_5 NWC is shown in Fig. 9(a, b) and cycled with the current density of 60 mA g^{-1} . The discharge capacity of the compound found to be decreasing with the increasing cycle number. However, we obtained a good capacity of 188 mAh g^{-1} with the better stability retention of around 90 % at the end of the 50th cycles for V_2O_5 NWC synthesized by gel-combustion using

cassava starch. Chen et al., have reported V_2O_5 precursor exhibited discharge capacity of $\sim 120 \text{mAh g}^{-1}$ in the initial cycle and $\sim 80 \text{mAh g}^{-1}$ at 30th cycle, in the potential range, 1.8 to 3.5 V with the current density, 29.5mA g^{-1} [46] and Tang et al. have reported sphere-like V_2O_5 nanoparticles cycled at 50mA g^{-1} with the voltage window of 2.0 - 4.0 V, had a discharge capacity of 106mAh g^{-1} at 50th cycle and an initial capacity of 262mAh g^{-1} also, the V_2O_5 nanoflowers exhibited, 87% capacity retention after 50th cycle (discharge capacity at 50th cycle, 239mAh g^{-1})[9]. Compared to the above literature, our V_2O_5 NWC behaves as a superior material on capacity and cycling stability performance. Moreover, the corresponding coulombic efficiency of 99 % was maintained during cycling which is shown in Fig. 9 (b).

A good C-rate performance is highly desirable in developing high power and fast charging lithium-ion batteries. The cycling response of V_2O_5 NWC at different C rates is shown in Fig. 10. When the C rates of the compound increases, thereversible capacity of the compound decreased. For example, the discharge capacities of V_2O_5 NWC at 35 (0.1C), 44 (0.15C), 88 (0.3C), 176 (0.6 C) 440 (1.5C) mA g^{-1} are 222, 169, 71, 32 and 17 mAh g^{-1} , respectively (1C= 294mA g^{-1} for 2 lithium ion). Even after deep cycling at 440mA g^{-1} , the NWC had 218mAh g^{-1} when the current is again reduced to 35mA g^{-1} .

To further investigate the kinetic properties of Li insertion and de-insertion of V_2O_5 NWC, the electrochemical impedance spectroscopy was carried out for fresh cell (open circuit voltage (OCV)), first charge (2.3, 2.5, 3.0, 3.5 and 4.0 V) and discharge (2.5, 2.3 and 2.0 V) at various voltages and after 50th cycle, at a current density of 60mA g^{-1} . Before measurement, the cell was kept at rest for 1 hour. Fig. 11 (a) shows the equivalent circuit, which is used to fit the impedance spectra of V_2O_5 NWC. The used equivalent circuit consists of resistance (electrolyte, surface film (sf), charge transfer (ct) and bulk resistance (b)), a constant phase element (CPEi) (sf, double layer (dI) and b which is used instead of pure capacitor due to the composite nature of the electrode), Warburg impedance (Ws) and

intercalation capacitance (C_i) [55-57]. The fitted individual impedance parameters are listed in Table 1. The fitted results were plotted as a Nyquist plot (real vs imaginary), shown in Fig. 12(a, b). In all the plots, the dotted line represents the experimental data and the straight line corresponds to fitted data. Fig. 11 (b) shows Nyquist plot of V_2O_5 NWC for fresh cell and after 50th cycle. The plots show only one semicircle in the high-mid frequency and straight line in the low frequency region. The electrolyte resistance (R_e) is found to be $6 (\pm 2) \Omega$. The charge transfer resistance (R_{sf+ct}) for fresh cell and after 50th cycle are found to be 115 and 88 (± 5) Ω , respectively. It is noted that, the kinetic energies of Li^+ are reduced after 50th cycles, indication of capacity fading, which is in good agreement with the cycling data. Fig. 12 (a, b) shows Nyquist plots of V_2O_5 NWC at various potentials for the first charge and discharge cycle. All plots in Fig. 12 (a, b) show, a single semi-circle in the high-mid frequency region, which is a combination of surface film and charge transfer resistance ($R_{(sf+ct)}$) and the corresponding $CPE_{(sf+dl)}$, where dl refers to double layer capacitance arises due to electrode/electrolyte interface. The electrolyte resistance was found to be almost same in all the plots, equals $5-7 (\pm 2) \Omega$. During discharging from 2.5-2.0 V, the resistance of the compounds started reducing, while charging from 2.5 to 4.0 V, the resistance reduced from 92-51 (± 5) Ω . The similar trend of the impedance for the first cycle different charge and discharge voltages was noted in the literature.

Conclusion

V_2O_5 nanowire clusters prepared by gel-combustion technique using cassava starch (*Manihot esculenta*) were investigated as possible cathode material for lithium ion batteries. The orthorhombic structure is confirmed from diffraction pattern for V_2O_5 compound, with the face group of *pmmn* (59). The scanning and transmission Electron Microscopic images revealed the V_2O_5 compound is in the form of nanowires and is closely packed like clusters

with the range of 100 nm. The V₂O₅ nanowire clusters exhibits a reversible capacity of 188 mAhg⁻¹, with the capacity retention of 90 % after 50th cycle. The increased capacity and better stability of the compound might be due to the effect of morphology.

Acknowledgement

The authors acknowledge Mr. K. Manjunath, JNCASR, India for the FTIR, UV and PL spectra and Institute of Excellence, University of Mysore for the SEM images.

References

1. A.Henglein, 'Small Particle Research: Physiochemical Properties of Extremely Small Colloidal Metal and Semiconductor Particles', *Chem Rev* 89, 1989, 1861-1873.
2. M. A. Zhen, B. Zhou, Y. Ren,'Crystallinemesoporous transition metal oxides: hard-templating synthesis and application in environmental catalysis, *Front. Environ. Sci. Eng.* 7, 2013, 341–355.
3. D. T. Gillaspie, R. C. Tenent, A. C. Dillon, 'Metal-oxide films for electrochromic applications: present technology and future directions', *J. Mater. Chem.* 20, 2010, 9585–9592.
4. J. Meyer , S. Hamwi , M. Kröger , W. Kowalsky , T. Riedl , A. Kahn,'Transition Metal Oxides for Organic Electronics: Energetics,Device Physics and Applications', *Adv. Mater.* 24, 2012, 5408–5427.
5. X. Xia, Y. Zhang, D. Chao, C. Guan, Y. Zhang, L. Li, X. Ge, I. M. Bacho, J. Tu, H. J. Fan, 'Solution synthesis of metal oxides for electrochemical energy storage applications', *Nanoscale* 6, 2014, 5008–5048.
6. N. Nitta, F. Wu, J. T. Lee, G. Yushin,'Li-ion Battery Materials: Present and Future', *Materials Today* 18, 2015, 252-264.
7. M. V. Reddy, G. V. SubbaRao, and B. V. R. Chowdari, 'Metal Oxides and Oxysalts as Anode Materials for Li Ion Batteries', *Chem. Rev.* 113, 2013, 5364–5457.

8. M. Sugawara, Y. Kitada, K. Matsuki, 'Molybdc Oxides as Cathode Active Materials In Secondary Lithium Batteries', *Journal of Power Sources* 26, 1989, 373–379.
9. Y. Tang, X. Rui, Y. Zhang, T. M. Lim, Z. Dong, H. H. Hng, X. Chen, Q. Yan, Z. Chen, 'Vanadium pentoxide cathode materials for high-performance lithium-ion batteries enabled by a hierarchical nanoflower structure via an electrochemical process', *J. Mater. Chem. A*, 2013, 1, 82-88.
10. N. A. Chernova, M. Roppolo, , A. C. Dillon, M. S. Whittingham, 'Layered vanadium and molybdenum oxides: batteries and electrochromics' *J. Mater. Chem.* 2009, 19, 2526-2552.
11. A. Sakunthala, M. V. Reddy, S. Selvasekarapandian, B. V. R. Chowdari, H. Nithya, P. C. Selvin, 'Synthesis and electrochemical studies on LiV₃O₈' *J. Solid State Electrochem.* 2010, 14, 1847-1854.
12. A. Sakunthala, M. V. Reddy, S. Selvasekarapandian, B. V. R. Chowdari, P. C. Selvin, 'Preparation, Characterization, and Electrochemical Performance of Lithium Trivanadate Rods by a Surfactant-Assisted Polymer Precursor Method for Lithium Batteries' *J. Phys. Chem. C*, 2010, 114, 8099-8107.
13. Ying Wang and Guozhong Cao, 'Synthesis and Enhanced Intercalation Properties of Nanostructured Vanadium Oxides', *Chem. Mater.* 2006, 18, 2787-2804.
14. A. Pan, J-G. Zhang, Z. Nie, G. Cao, B. W. Arey, G. Li, S-Q. Liang, J. Liu, 'Facile synthesized nanorodstructured vanadium pentoxide for high-rate lithium batteries', *J. Mater. Chem.* 20, 2010, 9193-9199.
15. M. G. Ancona, S. E. Kooi, W. Kruppa, A. W. Snow, E. E. Foos, L. J. Whitman, D. Park, L. Shirey, 'Patterning of Narrow Au Nanocluster Lines Using V₂O₅ Nanowire Masks and Ion-Beam Milling', *Nano Lett.* 3, 2003, 135-138.

16. L. Mai, L. Xu, C. Han, X. Xu, Y. Luo, S. Zhao, Y. Zhao, 'Electrospun Ultralong Hierarchical Vanadium Oxide Nanowires with High Performance for Lithium Ion Batteries', *Nano Lett.* **2010**, *10*, 4750–4755.
17. S-Z. Huang, Y. Cai, J. Jin, Y. Li, X.F. Zheng, H-E. Wang, M. Wu, L-H. Chen, B-L. Su, 'Annealed vanadium oxide nanowires and nanotubes as high performance cathode materials for lithium ion batteries', *J. Mater. Chem. A*, *2*, 2014, 14099–14108.
18. S.H. Ng, S.Y. Chewa, J. Wanga, D. Wexler, Y. Tournayre, K. Konstantinov, H.K. Liu, 'Synthesis and electrochemical properties of V₂O₅ nanostructures prepared via a precipitation process for lithium-ion battery cathodes', *Journal of Power Sources* *174*, 2007, 1032–1035.
19. D. Zhu, H. Liu, L. Lv, Y.D. Yao, W.Z. Yang, 'Hollow microspheres of V₂O₅ and Cu-doped V₂O₅ as cathode materials for lithium-ion batteries', *Scripta Materialia* *59*, 2008, 642–645.
20. W. Yu, J. Wang, Z. Gou, W. Zeng, W. Guo, L. Lin, 'Hydrothermal synthesis of vanadium pentoxide nanostructures and their morphology control' , *Ceramics International* *39*, 2013, 2639–2643.
21. T-D. Nguyen, T-O. Do, ' Solvo-Hydrothermal Approach for the Shape-Selective Synthesis of Vanadium Oxide Nanocrystals and Their Characterization, *Langmuir* *25*, 2009, 5322–5332.
22. Y. Wei, C-W. Ryub, K-B. Kimb, ' Cu-doped V₂O₅ as a high-energy density cathode material for rechargeable lithium batteries', *Journal of Alloys and Compounds* *459*, 2008, L13–L17.
23. Z.S. El Mandouh, M.S. Selim, 'Physical properties of vanadium pentoxide sol gel films', *Thin Solid Films* *371*, 2000, 259- 263.

24. A. Sakunthala, M. V. Reddy, S. Selvasekarapandian, B. V. R. Chowdari, P. C. Selvin, 'Energy storage studies of bare and doped vanadium pentoxide, (V_{1.95}M_{0.05})O₅, M = Nb, Ta, for lithium ion batteries' *Energy & Environmental Science* 2011, 4, 1712-1725.
25. M. E. A. Warwick, A. J. Roberts, R. C. T. Sladec, R. Binions, 'Electric field assisted chemical vapour deposition –a new method for the preparation of highly porous supercapacitor electrodes', *J. Mater. Chem. A*, 2, 2014, 6115–6120.
26. A. Gies, B. Pecquenard, A. Benayad, H. Martinez, D. Gonbeau, H. Fuess, A. Levasseur, 'Effect of silver co-sputtering on V₂O₅ thin films for lithium microbatteries' *Thin Solid Films*, 2008, 516, 7271-7281.
27. M. M. Rahman, A. Z. Sadek, I. Sultana, M. Srikanth, X. J. Dai, M. R. Field, D. G. Mcculloch, S. Ponraj, Y. Chen, 'Self-assembled V₂O₅ interconnected microspheres produced in a fish-water electrolyte medium as a high performance lithium-ion battery cathode', *Nano Research* 8, 2015, 3591-3603.
28. T. Miami, K.C. Patil, 'Solution combustion synthesis of nanoscale oxides and their composites', *Mater. Phys. Mech.* 4, 2001, 134–137.
29. Ed. M. Lackner, *Combustion Synthesis: Novel Routes to Novel Materials*, Bentham Science Publishers (2010).
30. Z. Cai, J. Li, 'Facile synthesis of single crystalline SnO₂ nanowires', *Ceramics International* 39 (2013) 377–382.
31. V. Savchyn, I. Karbovnyk, A.I. Popov, A. Huczko, *Combustion Formation of Novel Nanomaterials: Synthesis and Cathodoluminescence of Silicon Carbide Nanowires*, *ActaPhysicaPolonica A*, Vol. 116 (2009), 142- 145.
32. A. K. Ramasami, M. V. Reddy, G. R. Balakrishna, 'Combustion synthesis and characterization of NiO nanoparticles' *Mater. Sci. Semicond. Process.*, 2015, 40, 194-202.

33. Y. Sharma, N. Sharma, G. V. Subba Rao, B. V. R. Chowdari, 'Nanophase ZnCo₂O₄ as a high performance anode material for Li-ion batteries' *Adv. Funct. Mater.* 2007, 17, 2855-2861
34. M. V. Reddy, B. L. W. Wen, K. P. Loh, B. V. R. Chowdari, 'Energy Storage Studies on InVO₄ as High Performance Anode Material for Li-Ion Batteries' *ACS Appl. Mater. Interfaces* 2013, 5, 7777-7785.
35. G. Zhang, X. Shen, Y. Yang, Facile synthesis of monodisperse porous ZnO spheres by a soluble starch-assisted method and their photocatalytic activity, *J. Phys. Chem. C* 115, 2011, 7145–7152.
36. Gangulibabu, D. Bhuvaneswari, N. Kalaiselvi, 'Comparison of corn starch-assisted sol-gel and combustion methods to prepare LiM_nxCo_yNi_zO₂ compounds', *J Solid State Electrochem* 17, 2013, 9–17.
37. G. T-K. Fey, Y-D. Cho, T. Prem Kumar, 'A TEA-starch combustion method for the synthesis of fine-particulate LiMn₂O₄', *Materials Chemistry and Physics* 87, 2004, 275–284.
38. Y. L. Cheah, V. Aravindan S. Madhavi, 'Electrochemical Lithium Insertion Behavior of Combustion Synthesized V₂O₅ Cathodes for Lithium-Ion Batteries', *J. Electrochem. Soc.* 159, 2012, A273-A280.
39. A. Jagadeesh, T.M. Rattan, M. Muralikrishna, K. Venkataramaniah, 'Instant one step synthesis of crystalline nanoV₂O₅ by solution combustion method showing enhanced negative temperature coefficient of resistance', *Materials Letters* 121, 2014, 133–136.
40. S. Mishra, T. Rai, 'Morphology and functional properties of corn, potato and tapioca starches', *Food Hydrocolloids* 20, 2006, 557–566.

41. V. Tulyathan, K. Chimchom, K. Ratanathammapan, C. Pewlong, S. Navankasattusas, 'Determination of Starch Gelatinization Temperatures by Means of Polarized Light Intensity Detection' *J. Sci. Res. Chula. Univ.*1, 2006, 14-23.
42. G. Zhang, X. Shen, Y. Yang, 'Luminescence 3D-Ordered Porous Materials Composed of CdSe and CdTe Nanocrystals' *J. Phys. Chem. C* 115, 2011, 7145–7152.
43. A. K. Ramasami, H.R. Naika, H. Nagabhushana, T. Ramakrishnappa, G. R. Balakrishna, G. Nagaraju, 'Tapioca starch: An efficient fuel in gel-combustion synthesis of photocatalytically and anti-microbially active ZnO nanoparticles' *Materials Characterization* 99 (2015) 266–276.
44. J.J. Yu, J. Yang, W. B. Nie, Z. H. Li, E. H. Liu, G. T. Lei, Q. Z. Xiao, 'A porous vanadium pentoxide nanomaterial as cathode material for rechargeable lithium batteries', *Electrochimica Acta* 89, 2013, 292-299.
45. A. M. Cao, J. S. Hu, H.P. Liang, L. J. Wan, 'Self-Assembled Vanadium Pentoxide (V_2O_5) Hollow Microspheres from Nanorods and Their Application in Lithium-Ion Batteries', *Angew. Chem. Int. Ed.* 44, 2005, 4391-4395.
46. Y. Chen, G. Yang, Z. Zhang, X. Yang, W. Hou, J. J. Zhu, 'Polyaniline-intercalated layered vanadium oxide nanocomposites- One pot hydrothermal synthesis and application in lithium battery', *Nanoscale* 2, 2010, 2131-2138.
47. X. Zhou, C. Cui, G. Wu, H. Yang, J. Wu, J. Wang, G. Gao, 'A novel and facile way to synthesize vanadium pentoxide nanospikes as cathode material for high performance lithium ion batteries', *Journal of Power Sources* 238, 2013, 95-102.
48. Back G, Yu J-S, Lee H and Lee Y-III. Synthesis and spectroscopic characterization of vanadium incorporated V-*Al*MCM-41 molecular sieves. *Journal of the Korean Magnetic Resonance Society*. 2006; 10:141-154.

49. J. Tauc, (ed.), *Amorphous and Liquid Semiconductors*, New York, (1974) USA, Plenum Press.
50. C. V. Ramana, O. M. Hussain, 'Optical Absorption behaviour of vanadium pentoxide thin films', *Advanced materials for Optics and Electronics* 7, 1997, 225-231.
51. W. Avansi Jr, V. R. de Mendonca, O. F. Lopes, C. Rebeiro, 'Vanadium pentoxide 1-D nanostructures applied to dye removal from aqueous systems by coupling adsorption and visible light photodegradation', *RSC Adv* 5, 2015, 12000-12006.
52. A. Chakrabarti, K. Hermann, R. Druzinic, M. Witco, F. Wagner, M. Petersen, 'Geometric and Electronic structure of vanadium pentoxide: A density functional bulk and surface study', *Physical Review B* 59, 1999, 10583 - 10590.
53. M. Li, F. Kong, H. Wang, G. Li, 'Synthesis of vanadium pentoxide (V₂O₅) ultralong nanobelts via an oriented attachment growth mechanism', *CrystEngComm*, 13, 2011, 5317–5320.
54. C. Delmas, H. C. Auradou, J. M. Cocciantelli, M. Menetrier, J. P. Doumerc, 'The Li_xV₂O₅ system: An overview of the structure modifications induced by the lithium intercalation', *Solid State Ionics* 69, 1994, 257-264.
55. P. Nithyadharseni, M. V. Reddy, B. Nalini, M. Kalpana, B. V. R. Chowdari, 'Sn-based Intermetallic alloy anode materials for the application of lithium ion batteries', *Electrochimica Acta* 161, 2015, 261-268.
56. M. V. Reddy, G. V. Subba Rao, B. V. R. Chowdari, 'Nano-(V_{1/2}Sb_{1/2}Sn)O₄: a high capacity, high rate anode material for Li-ion batteries', *J. Mater. Chem* 21, 2011, 10003-10011.
57. P. Nithyadharseni, M. V. Reddy, Kenneth I. Ozoemena, R. Geetha Balakrishna, B. V. R. Chowdari, 'Low temperature molten salt synthesis of Y₂Sn₂O₇ anode material for lithium ion batteries', *Electrochimica Acta* 182, 2015, 1060-1069.

